euspen's 24th International Conference & Exhibition, Dublin, IE, June 2024
www.euspen.eu

High-efficiency fabrication of functional structured array surface on hard metallic ceramic materials by a novel magnetic field-assisted self-assembly electrode

K.S. Li[1], C.J. Wang[1*], C.F. Cheung[1], F. Gong[2]

[1]*State Key Laboratory of Ultra-precision Machining Technology, Department of Industrial and Systems Engineering The Hongkong Polytechnic University, Hong Kong, China*
[2]*Shenzhen Key Laboratory of High Performance Nontraditional Manufacturing, College of Mechatronics and Control Engineering Shenzhen University Shenzhen, Guangdong, China*

chunjin.wang@polyu.edu.hk (corresponding author)

Abstract

Hard metallic ceramic materials such as silicon carbide (SiC) and Tungsten carbide (WC), have been widely used in many important industrial applications attributing to their high hardness and stable material properties. Electrical discharge machining (EDM) is one of the effective methods to fabricate the functional structured surfaces on these materials. However, serious electrode wear together with a complicated electrode replacement process leads to high fabrication costs and low production efficiency. Hence, EDM with a self-assembly electrode was proposed for the fabrication of the functional structured array surface on metallic ceramic materials. Based on the discrete design concept, we designed a magnetic field-assisted self-assembly electrode (MASAE). The MASAE is made up of an array of ferromagnetic metallic balls attracted together under the guidance of the magnetic field generated by a permanent magnet. By adjusting the position, number, and size of the metallic balls, different MASAEs can be prepared. After the EDM process, different structured surface arrays on the metallic ceramic materials can be fabricated. The shape evolution and surface quality of the EDMed structure arrays were measured and analysed by ContourGT-X 3D optical profile and scanning electron microscope (SEM). The composition and phase changes of the EDMed surface were characterized by energy-dispersive X-ray spectroscopy (EDS) and Raman. Compared with the traditional integral electrodes made by milling or turning, the MASAE has a great advantage in preparation time, cost-effectiveness, and replaceability. The proposed manufacturing strategy provides an effective way for the design and manufacturing of functional structured surfaces on metallic ceramic materials.

Metallic ceramic materials; structured array surface; electrical discharge machining; self-assembly electrode

1. Introduction

Hard ceramic materials, such as binderless tungsten carbide (WC) and silicon carbide (SiC), are widely used in applications requiring high endurance and high temperature, such as semiconductor electronics devices, car parts, cutting tools, and moulds [1-3]. The effective machining of superhard ceramic materials is one of the research highlights for industry and academia. At present, energy-assisted precision cutting and grinding are two major traditional methods to fabricate functional structured array surfaces on metallic ceramic materials [4]. However, tool wear during the machining process strongly affects the manufacturing accuracy and surface integrity of the machined workpiece. Compared to traditional machining technology, electrical discharge machining (EDM) is one of the non-contact and non-traditional methods and has great advantages in machining hard and brittle materials [5-7].

In the EDM process, the design and development of the electrode is a crucial technique to improve manufacturing efficiency and fabricate a functional structured array surface. Xu et al. [8] used a micro-double-staged laminated object manufacturing method to prepare 3D micro-electrodes for micro-EDM. Yan et al. used a wheel-shaped rotary cupronickel electrode to complete the fabrication of a microstructure array on the polycrystalline diamond. Lei et al. [9] fabricated the deep-narrow blind microgroove array by EDM with a long-laminated electrode. Takino et al. [10] machined the spherical lens array by EDM with a ball-type electrode. Gu et al. [11] proposed a bundled die-sinking electrode to improve the machining efficiency of Ti6Al4V alloys. By designing and optimizing the electrodes during the EDM process, high-effeciency fabrication of functional structured array surfaces can be completed.

In this study, a novel MASAE is proposed for manufacturing of functional structured array surface on metallic ceramic materials. This MASAE is created by using a magnet to adsorb discrete balls. By adjusting the size of the magnet and balls, electrodes of different scales can be prepared. This flexibility in size customization allows for the fabrication of electrodes tailored to specific applications or machining requirements. Larger magnets and balls may be used to create electrodes suitable for machining larger workpieces or producing features on a macro scale. Conversely, smaller magnets and balls can be employed to fabricate electrodes for micro or nano-scale machining tasks. Furthermore, the shape evolution, removal rate, and surface quality of the WC and SiC surface after EDM with a MASAE are investigated. The composition and shape evolution of the EDMed surface are characterized. Finally, functional structured array surfaces with different shapes and sizes are fabricated.

2. Methods

2.1. Design and manufacture route

Based on the discrete design concept, we proposed a MASAE, as shown in Fig. 1(a). A self-assembly ball electrode is made up of magnet spheres with the help of the magnetic force of the permanent magnet. By tuning the arrangement and size of the balls, different self-assembly electrodes can be prepared. Fig. 1(b) shows the optical images of the SiC and WC structure array surface. By adjusting the position and number of magnetic balls, different ball array electrodes can be prepared. After the EDM process, different structured surface arrays on the superhard ceramic materials can be fabricated. Fig. 1(c) shows the SEM image and surface morphology of the EDMed structured surface.

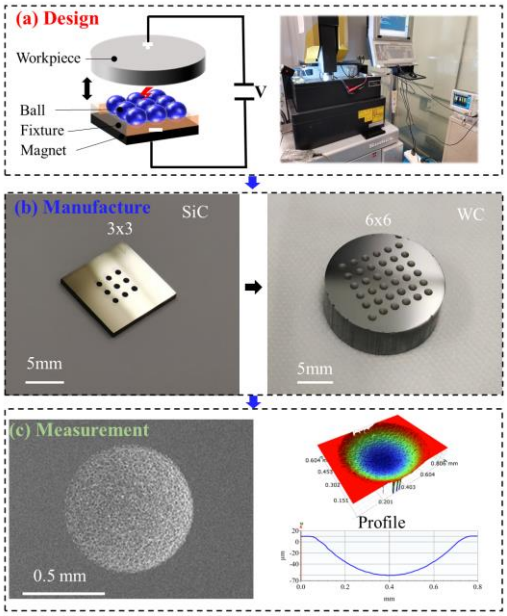

Figure 1. (a) The design principal of EDM with magnetic field-assisted self-assembly electrode, (b) The optical images of the SiC and WC structure array surface, (c) The measurement results of surface morphology.

2.2. Experimental section

Experiments were conducted on a Sodick electrical discharge machine (model AP1L) with three axes. Tungsten carbide (100 wt% WC, 0 wt% Co) and single-crystal 4H-SiC are chosen for the workpiece. By applying pulse energy between the electrodes and the workpiece, the surface structures of the self-assembly electrodes are transferred to the machined workpiece. The EDM conditions and properties of the electrodes are summarized in Table 1.

Table 1 EDM conditions

Conditions		**Value**
Processing parameters	Input current (A)	1
	Pulse width (μs)	1/5/10
	Pulse interval (μs)	10
	Open voltage (V)	105
	Dielectric fluid	Discharge oil
Tool electrodes	Tool diamater (mm)	1/2.4/3.2
	Resistivity (Ω.m)	$2x10^{-7}$
	Magnet (T)	1.1

2.3. Measurement and characterization

The surface roughness and shape evolution of the structured surface were measured by ContourGT-X 3D optical profiler (Bruker, Germany). The surface evolution of the structured array was observed using a scanning electron microscope (SEM, FEI, QUANTA FEG 450). The composition and phase changes of the EDMed surface were characterized by energy dispersive X-ray spectroscopy (EDS, FEI, QUANTA FEG 450) and Renishaw micro-Raman spectroscopy system (50 ×objective, laser beam size <10μm).

3. Results and discussions

3.1. Shape evolution and surface quality

Fig. 2 shows the surface morphology of the structured array made by EDM with a self-assembly ball electrode. The diameter and depth of the WC microlens array after EDM are about 450 μm and 47 um, respectively, as shown in Fig. 2(a). Fig. 2(b) shows the surface morphology of the SiC microlens array made by EDM with a self-assembly ball electrode. The diameter and depth of the SiC microlens array are about 425 μm and 50 μm, respectively. The difference in geometry size is due to the machining difficulty of different raw materials. The boiling points of WC and SiC are about 6000 ℃ and 2830 ℃, respectively. During the discharge process, the ablation local temperature can reach as high as 10000 K, significantly higher than the vaporization point of WC and SiC. Compared to the WC, the melting temperature of SiC is low, which affects the material removal rate during the EDM process.

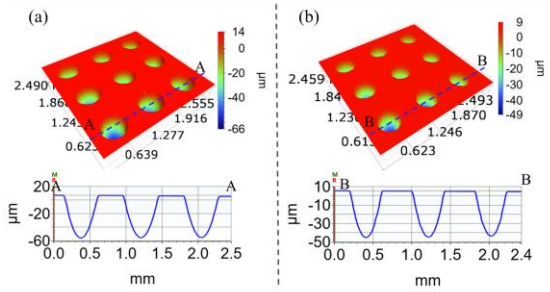

Figure 2. (a) The surface morphology of the EDMed WC surface, (b) The surface morphology of the EDMed SiC surface.

Fig. 3 shows the material removal rate (MRR), and tool wear ratio (TWR) during the EDM process. The MRR and TWR at different pulse widths when machining the WC substrate are shown in Fig. 3(a). When pulse widths are 1, 5, and 10 μs, the MRR are about 0.022 mm^3/min, 0.037 mm^3/min, and 0.052 mm^3/min under a constant pulse current of 1 A and pulse interval of 10 μs. In certain cases, the MRR and TWR increase as the pulse width increases. Fig. 3(b) shows the MRR and TWR at different pulse widths when machining the SiC substrate. It can be found that the rule of MRR in the machining process of SiC is similar to that of WC. However, the TWR in machining the SiC is less than that of WC. The maximum TWR when machining SiC substrate is less than 0.002 mm^3/min. The difference in TWR is also due to the differences in machining difficulty of different metallic ceramic materials.

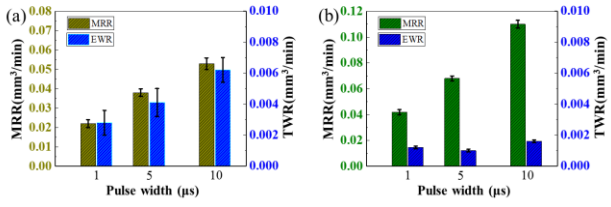

Figure 3. The MRR and TWR during EDM process (a) WC, (b) SiC.

Fig. 4 shows the SEM images of the EDMed surfaces. During discharge process, the interface between the workpiece and electrode forms a plasma channel and produces ultra-high instantaneous temperature, resulting in the melting and vaporization of the workpiece. After the EDM process, lots of ablation craters were formed in the EDMEd surfaces, as shown in Fig. 4(a). The micro-craters forming on the SiC surface affect the surface quality of the EDMed workpiece. Fig. 4(b) shows the SEM images of the WC structured array surface made by EDM with a self-assembly electrode. But unlike the SiC surface, lots of discharge micro-craters and microcracks can be observed on the EDMed WC surface. The tensile stress that occurs during rapid cooling is present in the resolidified layer of the WC surface, leading to the formation of microcracks.

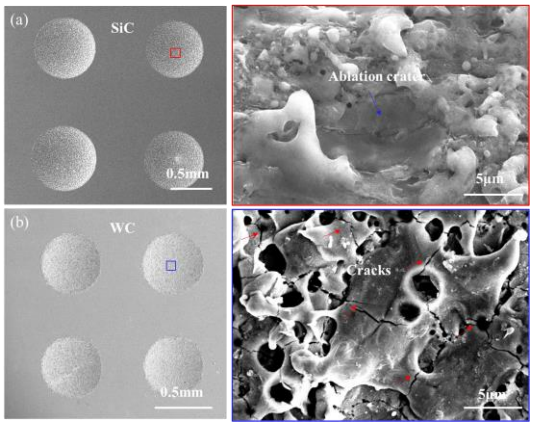

Figure 4. (a) The SEM images of the EDMed SiC surface, (b) The SEM images of the EDMed WC surface.

Fig. 5(a) shows the surface morphology of the EDMed SiC surface before and after curvature tilt. The surface arithmetic roughness (Sa) of the EDMed surface at different conditions is shown in Fig. 5(b) and (c). As the pulse width increases, larger micro-craters form on the fabricated surfaces, resulting in increased surface roughness. When the pulse width, interval, and current are 10 μs, 10 μs, and 1 A respectively, the Sa value of the EDMed WC surface approximates to 1.05 μm. Compared to the EDMed WC, the Sa of the EDMed SiC surface is larger. The maximum Sa of the EDMed SiC surface is about 1.23 μm. It is observed that the size of the discharge-induced craters on the SiC surface is larger than those on the WC surface, given the same discharge parameters. This explains why the surface roughness of the EDMed SiC surface is larger.

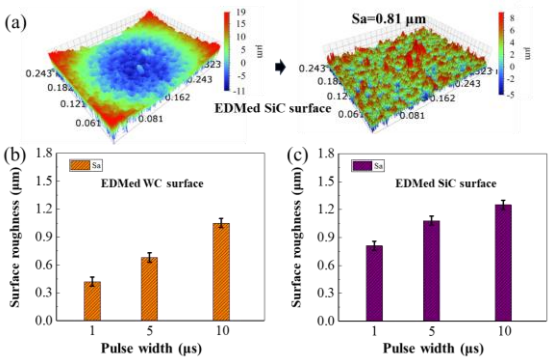

Figure 5. The surface quality after the EDM process (a) The surface morphology of the EDMed SiC surface, (b) The surface roughness of the EDMed WC at different pulse widths, (c) The surface roughness of the EDMed SiC at different pulse widths.

3.2. Composition and phase changes

Fig. 6 shows the SEM image and element distribution mapping of the EDMed SiC surface. It can be found that the C intensity of the C atom in the EDM region is stronger than that of the heat-affected region. The atom percentage of C is about 62%. After EDM, a small amount of O element can be observed. The atom percentage of O is about 2.7%. The formation of oxides during the EDM process is due to the high-temperature ablation effect. The oxides and carbonaceous are also found in the WC machining process [12]. During the vaporization-condensation process of SiC/WC, SiC/WC decomposes into Si/W and C and re-coagulates as separate elements.

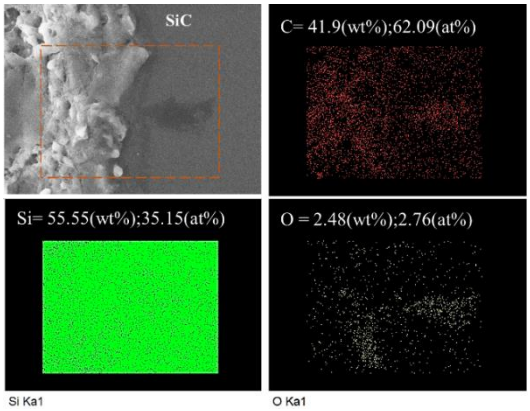

Figure 6. The composition and element changes of the EDMed SiC surface

Fig. 7 shows the Raman spectra in the 200-3200 cm^{-1} range obtained from the surfaces of WC and SiC before and after EDM. The D-band peaks at 1350 cm^{-1}, G-band peaks at 1587 cm^{-1} peaks and 2D-band peaks at 2700 cm^{-1} are detected after materials experience high-temperature discharge ablation. The D and G peaks are related to vibrations of carbon in the sp^2 and sp^3 bonds. The G-band is attributed to the stretching vibration of sp^2 atoms in rings and chains, while the D-band is associated with the breathing mode of sp^2 atoms in rings, and indicates the presence of disorder and defects in the hexagonal sp^2 structure. In Fig. 7(a), the D- and G-bands have not been found in the initial WC substrate. After EDM, very strong D- and G-band peaks are very apparent at the EDMed surface. Besides, graphene structure can also be detected, as shown in the insert image 2 of Fig. 7(a). The formation of carbon is due to the decomposition of WC.

Fig. 7(b) shows the Raman spectra and optical images of SiC surface before and after EDM. Before EDM, the SiC presents distinctive Raman peaks at 778 cm^{-1} and 971 cm^{-1}. After EDM, Raman peaks at 778 cm^{-1} and 971 cm^{-1} disappear, and a new peak at 521 cm^{-1} occurs, indicating the formation of crystalline SiC. Besides, very strong D- and G-band peaks can be found after EDM. The presence of Si and C implies the decomposition of SiC into Si and C. The intensity of the D-, G-, and 2D-bands serves as a measure to evaluate the degree of disorder in the graphitic structure. The EDMed SiC surface is a mixture of crystalline/amorphous Si, amorphous carbon and graphite/graphene. It can be concluded that due to the ultra-high temperature that occurred in the EDM process, SiC decomposes into Si and C, and re-coagulates as separate substances. The phase of carbon in the EDMed surface has graphite and amorphous structures. The phenomenon is similar to the structural changes of WC, but there are a few small changes.

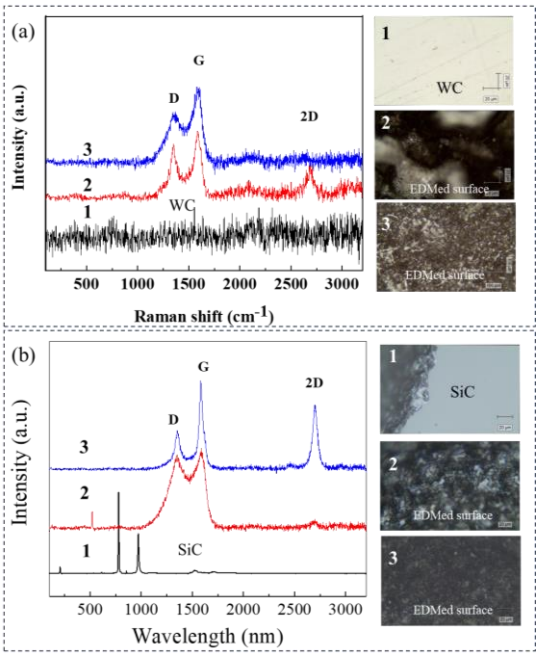

Figure 7. (a) The Raman spectrum and optical images of WC surface before and after EDM, (b) The Raman spectrum and optical images of SiC surface before and after EDM.

3.3. Different geometries of the structured array surfaces

Different depths and shapes of structured array surfaces on metallic ceramic materials can be fabricated by arranging the spherical balls in different arrays and controlling the discharge conditions. Fig. 8 (a) shows the different depths and diameters of structured array surfaces machined by self-assembly ball electrodes. The diameters of the structured array surfaces are about 0.3 mm, 1.2 mm, and 1.3 mm, respectively. Different diameters and depths of structured arrays on the WC and SiC are easily manufactured by adjusting the size of spherical balls and discharge parameters. Thus, self-assembly ball electrodes can be used to fabricate different kinds of freeform surface arrays.

Fig. 8(b) shows the structured array surfaces machined by self-assembly sheet electrodes. By adjusting the thickness and distance of the strip sheet, microstructure arrays with different sizes and shapes can be flexibly fabricated. In sum, the proposed EDM method is very convenient for the replacement of the electrode tool, which is cost-effective for the fabrication of structured array surfaces.

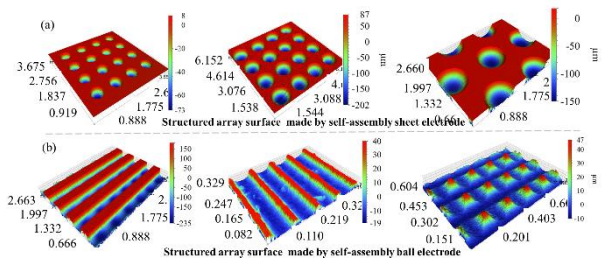

Figure 8. Functional structured array surface on metallic ceramic materials made by EDM with magnetic field-assisted self-assembly ball/sheet electrodes, (a) self-assembly ball electrodes, (b) self-assembly sheet electrodes.

4. Conclusions

In this paper, a novel MASAE for EDM of the structured array surfaces on metallic ceramic materials is presented. Compared with the traditional integral electrode made by milling or turning, MASAEs have a great advantage in fabricating the structured array surface on the SiC/WC substrates. Higher pulse energy can improve the machining efficiency and MRR during the EDM process, but it would induce the formation of larger craters, leading to increased surface roughness. Besides, SiC and WC decompose into Si/W and C, and then re-coagulate as separate substances due to the ultra-high temperatures generated during the EDM process. The EDMed surface is a mixture of carbon, oxides, and amorphous/crystalline substances, which changes the surface energy of initial materials. In conclusion, the work paves a new path for the design and fabrication of functional structured array surfaces on hard metallic ceramic materials.

Acknowledgement

The work described in this paper was mainly supported by a Shenzhen-Hong Kong-Macau Technology Research Programme from Shenzhen Science and Technology Innovation Committee (Project No: SGDX20220530110804030), the Research and Innovation Office of The Hong Kong Polytechnic University (Project code: BBR8 and BBX5), and Postdoctoral Matching Fund Scheme (1−W340). In addition, the authors would like to express their sincere thanks to the funding support from the Innovation and Technology Commission (ITC) of the Government of the Hong Kong Special Administrative Region (HKSAR), China (Project code: GHP/142/19SZ).

References

[1] Sun J, Zhao J, Huang Z, Yan K, Shen X, Xing J 2020 A Review on Binderless Tungsten Carbide: Development and Application *Nano-Micro Lett.* **12** 13-37.

[2] Zhao K, Fang P, Tan J, Zhong W, Liu J, Liu D 2023 A new route to fabricate high-performance binderless tungsten carbide: dynamic sinter forging *J. Am. Ceram. Soc.* **106** 3343-50.

[3] Nakamura D, Gunjishima I, Yamaguchi S, Ito T, Okamoto A, Kondo H, Onda S, Takatori K 2004 Ultrahigh-quality silicon carbide single crystals *Nature* **430** 1009–12.

[4] Liang X, Zhang C, Cheung CF, Wang C, Li K, Bulla B Micro/nano incremental material removal mechanisms in high-frequency ultrasonic vibration-assisted cutting of 316L stainless steel *Int. J. Mach. Tool. Manu.* **191** 104064.

[5] Ming WY, Xie ZB, Du JG, Zhang GJ, Cao C, Zhang Y 2021 Critical review on sustainable techniques in electrical discharge machining *J Manu. Process.* **72** 375-99.

[6] Jithin S, Joshi SS 2021 Surface topography generation and simulation in electrical discharge texturing: A review *J Mater. Process. Tech.* **298** 117297

[7] Philipp N, Richard L, Frank K, Rainer G 2015 Electrical discharge machining of metal doped Y-TZP/TiC nanocomposites *J. Eur. Ceram. Soc.* **35** 4031-7.

[8] Xu B, Wu X, Lei J, Cheng R, Ruan S, Wang Z 2015 Laminated fabrication of 3D micro-electrode based on WEDM and thermal diffusion welding *J. Mater. Process. Tech.* **221** 56-65.

[9] Lei J, Wu X, Zhou Z, Xu B, Tang Y 2021 Sustainable mass production of blind multi-microgrooves by EDM with a long-laminated electrode *J. Clean. Prod.* **279** 123492.

[10] Takino H, Hosaka T. 2016 Shaping of steel mold surface of lens array by electrical discharge machining with spherical ball electrode *Appl. Optics.* **55** 4967-73.

[11] Gu L, Li L, Zhao W, Rajurkar KP. 2012 Electrical discharge machining of Ti6Al4V with a bundled electrode *Int. J. Mach. Tool. Manu.* **53** 100-6.

[12] Li K, Wang C, Gong F, Cheung CF. 2023 Facile and flexible fabrication of structured array surfaces on binderless tungsten carbide by using electrical discharge machining with a novel self-assembly ball electrode *J. Am. Ceram. Soc.* **106** 7386-99.